

Double Superconducting Dome and Triple Enhancement of T_c in the Kagome Superconductor CsV_3Sb_5 under High Pressure

K. Y. Chen^{1,2,*} N. N. Wang^{1,2,*} Q. W. Yin^{3,*} Y. H. Gu^{1,2} K. Jiang^{1,2} Z. J. Tu³
C. S. Gong³ Y. Uwatoko⁴ J. P. Sun^{1,2,†} H. C. Lei^{3,‡} J. P. Hu^{1,2} and J.-G. Cheng^{1,2,§}

¹Beijing National Laboratory for Condensed Matter Physics and Institute of Physics, Chinese Academy of Sciences, Beijing 100190, China

²School of Physical Sciences, University of Chinese Academy of Sciences, Beijing 100190, China

³Department of Physics and Beijing Key Laboratory of Opto-electronic Functional Materials & Micro-nano Devices, Renmin University of China, Beijing 100872, China

⁴Institute for Solid State Physics, University of Tokyo, Kashiwa, Chiba 277-8581, Japan



(Received 28 February 2021; accepted 18 May 2021; published 17 June 2021)

CsV_3Sb_5 is a newly discovered Z_2 topological kagome metal showing the coexistence of a charge-density-wave (CDW)-like order at $T^* = 94$ K and superconductivity (SC) at $T_c = 2.5$ K at ambient pressure. Here, we study the interplay between CDW and SC in CsV_3Sb_5 via measurements of resistivity, dc and ac magnetic susceptibility under various pressures up to 6.6 GPa. We find that the CDW transition decreases with pressure and experience a subtle modification at $P_{c1} \approx 0.6$ – 0.9 GPa before it vanishes completely at $P_{c2} \approx 2$ GPa. Correspondingly, $T_c(P)$ displays an unusual M -shaped double dome with two maxima around P_{c1} and P_{c2} , respectively, leading to a tripled enhancement of T_c to about 8 K at 2 GPa. The obtained temperature-pressure phase diagram resembles those of unconventional superconductors, illustrating an intimated competition between CDW-like order and SC. The competition is found to be particularly strong for the intermediate pressure range $P_{c1} \leq P \leq P_{c2}$ as evidenced by the broad superconducting transition and reduced superconducting volume fraction. The modification of CDW order around P_{c1} has been discussed based on the band structure calculations. This work not only demonstrates the potential to raise T_c of the V-based kagome superconductors, but also offers more insights into the rich physics related to the electron correlations in this novel family of topological kagome metals.

DOI: 10.1103/PhysRevLett.126.247001

The newly discovered kagome metals AV_3Sb_5 ($A = \text{K}, \text{Rb}, \text{Cs}$) have aroused tremendous research interest as a novel platform to study the interplay between nontrivial band topology, superconductivity (SC), and charge-density-wave (CDW) order [1–4]. At ambient conditions, these materials crystallize into a layered structure with hexagonal symmetry (space group $P6/mmm$), inset of Fig. 1(a), consisting of A layer and V-Sb slab stacked alternatively along the c axis [1]. The most prominent feature of this structure is the presence of quasi-2D ideal kagome layers of V ions coordinated by Sb. These compounds are metallic and enter a superconducting ground state below $T_c = 0.93, 0.92,$ and 2.5 K for $A = \text{K}, \text{Rb},$ and Cs [2–4], respectively. Recent measurements of thermal conductivity on CsV_3Sb_5 single crystals at ultralow temperatures evidenced a finite residual linear term, pointing to an unconventional nodal SC [5]. In addition, proximity-induced spin-triplet SC and edge supercurrent were reported in the $\text{Nb}/\text{K}_{1-x}\text{V}_3\text{Sb}_5$ devices [6]. In the normal state, their transport and magnetic properties exhibit a clear anomaly at $T^* = 78, 104,$ and 94 K, respectively, due to the

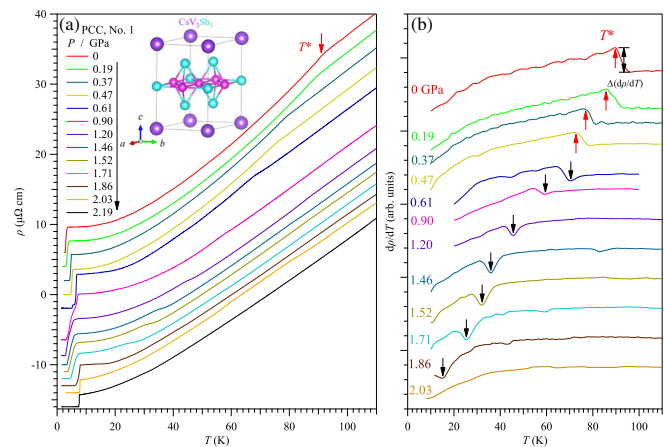


FIG. 1. Variation with pressure of the CDW-like transition. Temperature dependences of (a) resistivity $\rho(T)$ and (b) its derivative $d\rho/dT$ for the CsV_3Sb_5 sample No. 1 measured in PCC under various pressures up to 2.2 GPa. Inset of (a) shows the crystal structure of CsV_3Sb_5 . The transition temperature of CDW-like order, T^* , are marked by the arrows in the figures. The curves in (a),(b) have been shifted vertically for clarity.

formation of CDW-like order as revealed by the x-ray diffraction and scanning tunneling microscopy measurements [2–4,7]. The charge order in KV_3Sb_5 has been found to display a chiral anisotropy [7], which can lead to a giant anomalous Hall effect in the absence of magnetic order or local moments [8,9]. It was also argued as a strong precursor of unconventional SC [7]. Moreover, angle-resolved photoemission spectroscopy measurements and density-functional-theory calculations have characterized their normal state as a Z_2 topological metal with multiple Dirac nodal points near the Fermi level [1,4], consistent with the observations of Shubnikov–de Haas quantum oscillations and small Fermi surfaces (FSs) with low effective mass in RbV_3Sb_5 [3].

At present, the topologically related phenomena and SC have been actively studied in these AV_3Sb_5 compounds [10–35], but the possible rich physics related to the electron correlation, especially the relationship between the intertwined electronic orders [36,37], has been barely revealed. In this regard, it is interesting to unveil the correlation between the CDW-like order and SC commonly observed in these AV_3Sb_5 materials. Here, we have chosen to study CsV_3Sb_5 with the highest T_c among this series of compounds by applying a high-pressure approach, which has been widely used in disentangling the competing electronic orders of strongly correlated metals [38]. Through detailed measurements of resistivity, dc and ac magnetic susceptibility under various pressures, we successfully uncover an *M*-shaped double superconducting dome associated with the modification of the CDW-like order and the subsequent suppression under pressure. Interestingly, the T_c of CsV_3Sb_5 is almost triply enhanced to about 8 K at 2 GPa, which should inspire more interest to further raise T_c of these V-based kagome superconductors. By revealing the coexistence and competition of SC with the CDW order in the temperature-pressure phase diagram of CsV_3Sb_5 , our results provide more insights into the rich correlation-related physics pertinent to this novel family of kagome metals.

Single crystals of CsV_3Sb_5 were grown with the self-flux method [3]. Temperature dependences of resistivity, $\rho(T)$, for two samples (No. 1, No. 2) and ac magnetic susceptibility, $\chi'(T)$, for sample No. 3 were measured simultaneously with a piston cylinder cell (PCC) under various pressures up to 2.2 GPa [39]. Daphne 7373 was used as the pressure transmitting medium (PTM). The pressure in PCC was determined from the superconducting transition of Pb according to the equation: $P(\text{GPa}) = (T_0 - T_c)/0.365$, where $T_0 = 7.20$ K is the T_c of Pb at ambient pressure. We also measured $\rho(T)$ on sample No. 4 up to 6.6 GPa with cubic anvil cell (CAC) [40], in which glycerol was employed as PTM. dc magnetization measurements on sample No. 5 up to 0.87 GPa were performed with a miniature BeCu PCC fitted into the commercial Magnetic Property Measurement System (Quantum Design). Details

about the crystal growth, structure, chemical composition, and high-pressure measurements are given in the Supplemental Material (SM) [41].

Figures 1(a) and 1(b) show the $\rho(T)$ and its derivative $d\rho/dT$ of sample No. 1 under various pressures up to 2.2 GPa. These data illustrate clearly how the CDW-like order evolve with pressure. At 0 GPa, the CDW transition at $T^* \approx 94$ K is manifested as a kinklike anomaly in $\rho(T)$ and a corresponding peak in $d\rho/dT$. With increasing pressure, T^* moves to lower temperatures and reaches about 15 K at 1.86 GPa, above which it cannot be discerned in $\rho(T)$, implying a complete suppression of the CDW-like order by pressure. It is noteworthy that the kinklike feature in $\rho(T)$ at T^* is diminished at 0.6–0.9 GPa and changes at higher pressures to a humplike anomaly, Fig. 1(a), which is similar with that of KV_3Sb_5 at ambient pressure [13]. This is a typical character of CDW formation associated with the gap opening over part of the FSs [50–52]. Accordingly, the anomaly in $d\rho/dT$ changes from a peak for $P < 0.6$ GPa through an intermediate crossover region to a dip for $P > 0.9$ GPa as shown in Fig. 1(b). These observations are confirmed in sample No. 2 as shown in Fig. S3 of SM. These results indicate that the CDW-like order undergoes a subtle modification and might evolve into a distinct CDW state at $P > 0.9$ GPa. Such a change in the normal state has a profound impact on the superconducting transition as shown below.

Figure 2(a) displays an enlarged view of the above $\rho(T)$ data below 10 K, highlighting a complex, nonmonotonic variation with pressure of the superconducting transition. The T_c^{onset} is determined from the cross point of two straight lines above and below the transition, while T_c^{zero} is defined as zero-resistance temperature. The $\rho(T)$ at 0 GPa shows a relatively sharp superconducting transition with $T_c^{\text{onset}} \approx 3.5$ K and $T_c^{\text{zero}} \approx 2.8$ K, consistent with the previous result [4,5]. With increasing pressure, T_c^{onset} and T_c^{zero} are raised up to about 5 and 4.3 K at 0.37 GPa, and to about 6.8 and 5 K at 0.61 GPa, respectively. At 0.61 GPa, there exists a small step before reaching zero resistivity, indicating the presence of two superconducting phases. Such a feature evolves into a quite broad transition at 0.9 GPa with $T_c^{\text{onset}} \approx 7.2$ K and $T_c^{\text{zero}} \approx 3$ K. When applying pressure to 1.2 GPa, the normal-state resistivity is reduced, and the broad-shoulder feature is weakened by reducing T_c^{onset} to 5.7 K while leaving T_c^{zero} at 2.8 K. But the transition width $\Delta T_c \approx 3$ K is still large. Interestingly, T_c is shifted again to higher temperatures upon further increasing pressure; i.e., T_c^{onset} and T_c^{zero} at 1.86 GPa reaches about 8 and 6 K, respectively. In the pressure range of 1.2–1.86 GPa, $\Delta T_c \approx 2$ –3 K remains large due to either a broad onset or a long tail upon approaching zero.

When the CDW-like order just vanishes at ~ 2 GPa, the superconducting transition becomes very sharp with a $\Delta T_c \approx 0.3$ K. As seen in Fig. 2(a), T_c^{onset} and T_c^{zero} are 7.96 and 7.63 K for 2.03 GPa, and 7.68 and 7.43 K for

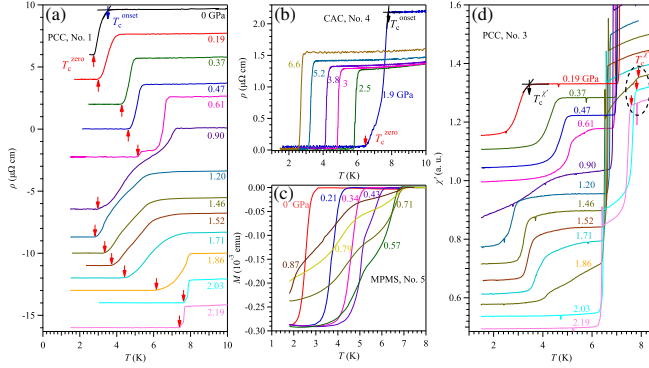


FIG. 2. Variation with pressure of the superconducting transition in (a),(b) resistivity and (c),(d) magnetic susceptibility. The resistivity $\rho(T)$ data in (a) and (b) are measured for sample No. 1 up to 2.2 GPa with PCC and for sample No. 4 up to 6.6 GPa with CAC, respectively. The dc magnetization in (c) was recorded in MPMS on sample No. 5 with a miniature PCC, while the ac magnetic susceptibility in (d) was measured on sample No. 3 with the mutual induction method in PCC.

2.19 GPa, respectively. It seems that T_c will decrease at higher pressures, which is further tracked by measuring $\rho(T)$ on sample No. 4 with CAC. As seen in Fig. 2(b), the $\rho(T)$ at 1.9 GPa in CAC resembles that of 1.86 GPa in PCC, showing a relatively sharp onset but a long tail with $T_c^{\text{onset}} \approx 7.8$ K and $T_c^{\text{zero}} \approx 6.5$ K. For $P \geq 2.5$ GPa, the superconducting transition becomes very sharp with $\Delta T_c \approx 0.3$ K and shifts to lower temperatures monotonically. T_c^{onset} and T_c^{zero} are reduced to 2.82 and 2.58 K at 6.6 GPa.

Since $T_c(P)$ exhibits a complex variation with pressure and the ΔT_c is quite large in the intermediate pressure range 0.6–1.9 GPa where the CDW order coexists, it is essential to further characterize the superconducting transition via magnetic measurements. Figure 2(c) shows the dc magnetization $M(T)$ of sample No. 5 up to 0.87 GPa measured upon warming up under $H = 5$ Oe after zero-field-cooled from room temperature. The diamagnetic signal appears at $T_c^M = 2.5$ K for 0 GPa, in agreement with the $\rho(T)$ data, and it moves quickly to ~ 6.5 K at 0.71 GPa. For $P < 0.7$ GPa, the bulk nature of SC is confirmed by the large diamagnetic response in $M(T)$. For $P > 0.7$ GPa, the diamagnetic responses appear at high temperatures of 6–7 K, but the transition is very broad and its magnitude is also lowered. This suggests that the superconducting volume fraction is reduced, consistent with the broad transition in $\rho(T)$ at similar pressures as shown in Fig. 2(a).

The ac susceptibility $\chi'(T)$ of sample No. 3 up to 2.2 GPa, Fig. 2(d), show one-to-one correspondence to the $\rho(T)$ shown in Fig. 2(a), including the two-step feature of the superconducting transition at 0.61 and 0.9 GPa, the reduction of T_c from 0.6 to 1.2 GPa followed by a resurgence of T_c up to 1.86 GPa with a relatively broad transition, and a sharp transition at $P \geq 2$ GPa. The abrupt

drop of $\chi'(T)$ around 7 K is due to the superconducting transition of Pb, which decreases with pressure. By comparing the diamagnetic signals of Pb and CsV_3Sb_5 with known volume, the superconducting shielding volume fraction of CsV_3Sb_5 can be estimated and is found to be relatively small, $\sim 30\%$ – 50% , for $0.6 \leq P \leq 1.86$ GPa when the CDW order coexists, while a nearly 100% bulk SC is realized at 2 GPa when the CDW order vanishes completely. These results thus provide direct evidence for the microscopic coexistence and competition between CDW and SC [53].

Based on the above comprehensive high-pressure characterizations, we construct the T - P phase diagram of CsV_3Sb_5 , Figs. 3(a) and 3(b), which depicts explicitly the evolutions and correlations of T^* and T_c as a function of pressure. As can be seen, $T^*(P)$ decreases monotonically with pressure and vanishes completely around $P_{c2} \approx 2$ GPa, while $T_c(P)$ displays an M -shaped double dome character with two maxima around $P_{c1} \approx 0.6$ – 0.9 GPa and P_{c2} , respectively. The highest $T_c \approx 8$ K is achieved around P_{c2} and it is nearly three times higher than that at ambient pressure. This observation immediately calls attention to further raise the T_c of these V-based kagome superconductors. It is noted that samples No. 1 and No. 2 display nearly identical behaviors of $T^*(P)$, $T_c(P)$, and $\Delta T_c(P)$ even though they show different levels of intrinsic disorder, as indicated by the different values of residual resistivity ratio, i.e., $RRR = \rho(280 \text{ K})/\rho(5 \text{ K}) = 43$ for No. 1 and 22 for No. 2, respectively. These results indicate that the intrinsic disorders within a certain range for our studied samples play a marginal role for the above observations under pressure.

The major finding of the present work is the observation of an M -shaped double superconducting dome, which does not arise from the sample inhomogeneity (see SM for detailed characterizations), but has an intimated correlation with the high-temperature CDW-like order. As pointed out above, the $\rho(T)$ anomaly around T^* displays a subtle change from a kinklike rapid reduction at $P < 0.6$ GPa to a humplike weak upturn at $P > 0.9$ GPa through an intermediate crossover region. Accordingly, the anomaly in $d\rho/dT$ around T^* changes from a peak to a dip, Fig. 1(b). To illustrate such a change, the symbols of T^* and the area below in Fig. 3(a) are color coded in terms of the sign of $\Delta(d\rho/dT)$ at T^* as defined in Fig. 1(b), which shows a clear sign reversal around P_{c1} . As mentioned above, the weak upturn of $\rho(T)$ upon cooling across T^* at $P_{c1} \leq P \leq P_{c2}$ is a typical character for the formation of CDW-like state that opens a gap over part of FSs. But the CDW order at $P_{c1} \leq P \leq P_{c2}$ should be distinct from that at ambient pressure given the different responses of $\rho(T)$ at T^* . This new CDW order shows a stronger tendency to compete with SC [53,54], featured by broad superconducting transitions and reduced superconducting volume fraction at $P_{c1} \leq P \leq P_{c2}$. As a result, the suppression of CDW

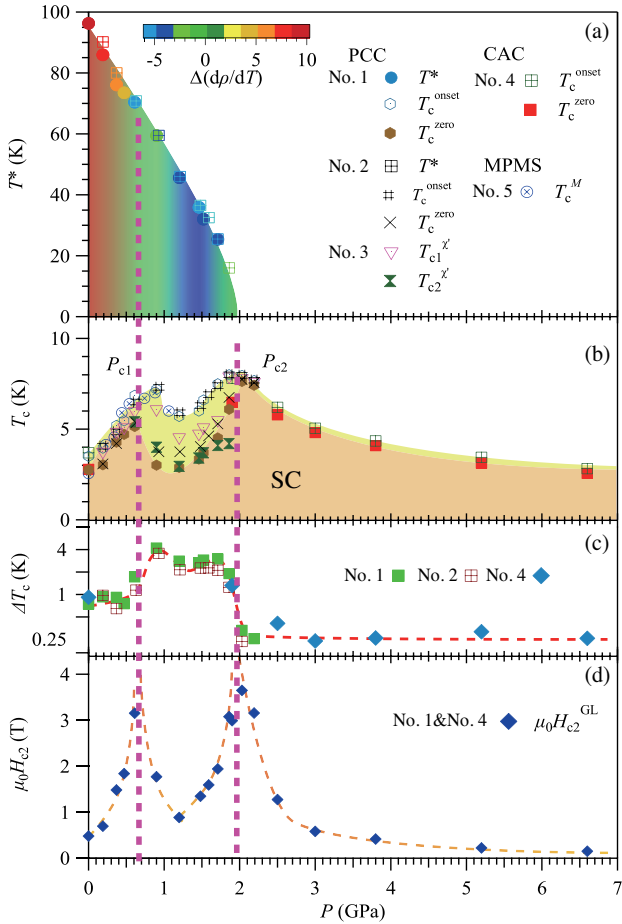


FIG. 3. Temperature-pressure phase diagram of CsV_3Sb_5 . Pressure dependences of (a) the CDW-like transition temperature T^* , (b) the superconducting transition temperatures T_c^{onset} , T_c^{zero} , T_c^M , and T_c^* determined from the resistivity and magnetic measurements on several samples, (c) the superconducting transition width ΔT_c , and (d) the zero-temperature upper critical field $\mu_0 H_{c2}(0)$ obtained from the empirical Ginzburg-Landau (GL) fitting.

order by pressure leads to an initial enhancement of T_c , but the modification of the CDW order around P_{c1} with a stronger competition with SC produces the first extremum of T_c shown in Fig. 3(b).

The continuous suppression of CDW order by pressure results in the resurgence of SC at higher pressures, giving rise to a second extremum of T_c around P_{c2} when the CDW order just vanishes. The observed maximal T_c in the vicinity of P_{c2} followed by a subsequent monotonic reduction of T_c at higher pressures resembles those of many unconventional superconducting systems characterized by the presence of quantum criticality [38,55–60]. To examine such a possibility, we probe the evolution of the electronic states by evaluating the upper critical field, $\mu_0 H_{c2}$, of the superconducting state as detailed in Figs. S5–S7 of SM. The extracted zero-temperature $\mu_0 H_{c2}(0)$ based on the Ginzburg-Landau fitting are plotted

in Fig. 3(d) as a function of pressure. Interestingly, the $\mu_0 H_{c2}(0)$ displays two pronounced peaks around P_{c1} and P_{c2} , respectively. The corresponding $\mu_0 H_{c2}(0)$ values are larger than 3 T, about one order of magnitude higher than that at ambient pressure. Similar double-peak features are also observed in the pressure dependence of the initial slope of $\mu_0 H_{c2}(T)$, i.e., $-dH_{c2}/dT|_{T_c}$, which is proportional to the effective mass of charge carriers [42]. The divergence behaviors of $-dH_{c2}/dT|_{T_c}$ around P_{c2} signal the dramatic enhancement of effective mass, which has been regarded as a hallmark of quantum criticality [43]. The presence of quantum criticality around P_{c2} is conceivable due to complete suppression of the CDW order, in line with many unconventional superconductors [61–66]. However, whether there is a buried quantum critical point (QCP) around P_{c1} deserves further investigations.

To unveil the nature of the subtle change of CDW order around P_{c1} , we carried out density-functional-theory calculations on CsV_3Sb_5 under pressure. The computational details are given in the SM. From the electronic structure without pressure shown in Fig. 4(a) and previous reports [1,4], the CsV_3Sb_5 is a quasi-2D metal with multiple cylinder FSs. The FS around the Γ point is mainly coming from the in-plane Sb p_z orbital and the FSs around the M point are coming from the V d orbitals. The CDW phase is widely believed from the scattering between M point van

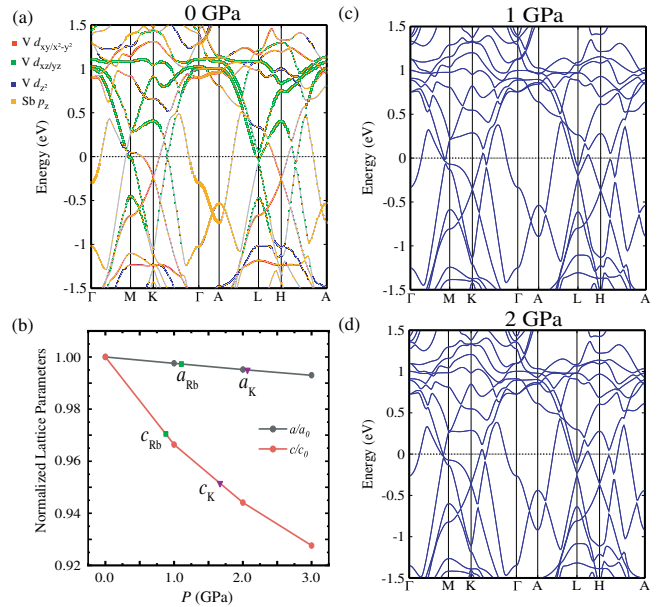


FIG. 4. (a) Band structure of CsV_3Sb_5 without external pressure. The orbital characters of bands are represented by different colors and the projected weights are represented by the sizes. (b) Normalized lattice constants as a function of pressure for CsV_3Sb_5 . The optimized lattice constants of RbV_3Sb_5 and KV_3Sb_5 without pressure are represented by green squares and purple triangles and the corresponding “chemical pressures” are calculated by linear extrapolation. Band structure of CsV_3Sb_5 under external pressure of (c) 1 GPa and (d) 2 GPa.

Hove (VH) singularity. As adding pressure to the system, the c axis is compressed much faster than the a axis, as shown in Fig. 4(b). So the electronic structure becomes more dispersive in the c axis at higher pressures. Since the ion radius $r_{\text{Cs}} > r_{\text{Rb}} > r_{\text{K}}$, the ion substitution is equivalent to changing pressure as indicated in Fig. 4(b). Because of its quasi-2D nature, it is highly possible that the correlation interaction between the layers in CsV_3Sb_5 force the CDW order from VH singularity to develop a nonvanishing order wave vector along the c axis. When the dispersion along the c axis increases under pressure so as to weaken the nesting scattering effect, the vanishing of this out-of-plane wave vector along the c axis takes place and gives rise to the first SC dome around P_{c1} . This additional CDW transition also explains the change of $d\rho/dT$ anomaly around T^* found in Fig. 1. For KV_3Sb_5 , the electronic structure is more dispersive in the c direction, which may explain the single superconducting dome under pressure and the smaller critical pressure [13].

Finally, we would like to comment briefly that the distinct superconducting dome behaviors and $\mu_0 H_{c2}$ values observed in this work and those in Ref. [5] employing diamond anvil cell (DAC) should be mainly attributed to the different high-pressure techniques. Here, the employed PCC and CAC with liquid PTM can maintain a relatively good hydrostatic pressure condition, making it possible to track the evolution of the CDW order from resistivity and thus allowing us to establish a comprehensive T - P phase diagram shown in Fig. 3. However, the pressure capacity of CAC is not high enough to access the second superconducting phase (SC-II) above 15 GPa reported in Ref. [5]. In contrast, the sample in DAC filled with solid or even no PTM is expected to experience a severe pressure inhomogeneity. As such, the superconducting transition is broad and the CDW order cannot be detected from the resistance measurements, resulting in a different phase diagram. Nonetheless, the large pressure capacity of DAC enabled the discovery of the SC-II phase above 15 GPa [5].

In summary, we performed a comprehensive high-pressure study on the newly discovered Z_2 topological kagome metal CsV_3Sb_5 , which shows the coexistence of CDW-like order and SC at ambient pressure. Our results uncover a hitherto unknown pressure-induced modification of the CDW order around $P_{c1} \approx 0.6 - 0.9$ GPa before it is completely suppressed around $P_{c2} \approx 2$ GPa. Accordingly, $T_c(P)$ exhibits an M -shaped double superconducting dome with two maxima located at P_{c1} and P_{c2} , respectively, thus revealing an intimated interplay between CDW and SC. The T_c of CsV_3Sb_5 is almost triply enhanced to 8 K at 2 GPa, implying that the T_c of these V-based kagome superconductors has room to go higher. In addition, the double-peak character is also observed in $\mu_0 H_{c2}(0)$, and characteristics of quantum criticality are also indicated. The determined T - P phase diagram with a quantum criticality around P_{c2} resembles those of many unconventional

superconductors, thus providing more ingredients related with the strong electron correlations into the rich physics of this novel family of topological kagome metals. Several open issues, such as the nature of the CDW-like order at $P_{c1} \leq P \leq P_{c2}$ and the plausible buried QCP around P_{c1} , still need to be addressed in future studies.

This work is supported by the National Natural Science Foundation of China (Grants No. 12025408, No. 11888101, No. 11904391, No. 11921004, No. 11834016, No. 11822412, and No. 11774423), the Beijing Natural Science Foundation (Grants No. Z190008 and No. Z200005), the National Key R&D Program of China (Grants No. 2018YFA0305700, No. 2018YFE0202600, and No. 2016YFA0300504), the Strategic Priority Research Program and Key Research Program of Frontier Sciences of the Chinese Academy of Sciences (Grants No. XDB25000000, No. XDB33000000, and No. QYZDB-SSW-SLH013), and the CAS Interdisciplinary Innovation Team. U. W. is supported by the JSPS KAKENHI Grant No. 19H00648. Some high-pressure experiments were carried out at the Synergic Extreme Condition User Facility.

*These authors contributed equally to this work.

†jpsun@iphy.ac.cn

‡hlel@ruc.edu.cn

§jgcheng@iphy.ac.cn

- [1] B. R. Ortiz, L. C. Gomes, J. R. Morey, M. Winiarski, M. Bordelon, J. S. Mangum, I. W. H. Oswald, J. A. Rodriguez-Rivera, J. R. Neilson, S. D. Wilson, E. Ertekin, T. M. McQueen, and E. S. Toberer, New kagome prototype materials: Discovery of KV_3Sb_5 , RbV_3Sb_5 , and CsV_3Sb_5 , *Phys. Rev. Mater.* **3**, 094407 (2019).
- [2] B. R. Ortiz, E. Kenney, P. M. Sarte, S. M. L. Teicher, R. Seshadri, M. J. Graf, and S. D. Wilson, Superconductivity in the Z_2 kagome metal KV_3Sb_5 , *Phys. Rev. Mater.* **5**, 034801 (2021).
- [3] Q. W. Yin, Z. J. Tu, C. S. Gong, Y. Fu, S. H. Yan, and H. C. Lei, Superconductivity and normal-state properties of kagome metal RbV_3Sb_5 single crystals, *Chin. Phys. Lett.* **38**, 037403 (2021).
- [4] B. R. Ortiz, S. M. L. Teicher, Y. Hu, J. L. Zuo, P. M. Sarte, E. C. Schueller, A. M. M. Abeykoon, M. J. Krogstad, S. Rosenkranz, R. Osborn, R. Seshadri, L. Balents, J. He, and S. D. Wilson, CsV_3Sb_5 : A Z_2 Topological Kagome Metal with a Superconducting Ground State, *Phys. Rev. Lett.* **125**, 247002 (2020).
- [5] C. C. Zhao, L. S. Wang, W. Xia, Q. W. Yin, J. M. Ni, Y. Y. Huang, C. P. Tu, Z. C. Tao, Z. J. Tu, C. S. Gong, H. C. Lei, Y. F. Guo, X. F. Yang, and S. Y. Li, Nodal superconductivity and superconducting dome in the topological kagome metal CsV_3Sb_5 , *arXiv:2102.08356*.
- [6] Y. J. Wang, S. Y. Yang, P. K. Sivakumar, B. R. Ortiz, S. M. L. Teicher, H. Wu, A. K. Srivastava, C. Garg, D. F. Liu, S. S. P. Parkin, E. S. Toberer, T. McQueen, S. D. Wilson, and M. N. Ali, Proximity-induced spin-triplet

- superconductivity and edge supercurrent in the topological kagome metal, $K_{1-x}V_3Sb_5$, [arXiv:2012.05898](#).
- [7] Y. X. Jiang, J. X. Yin, M. M. Denner, N. Shumiya, B. R. Ortiz, J. Y. He, X. X. Liu, S. S. Zhang, G. Q. Chang, I. Belopolski, Q. Zhang, M. Shafayat Hossain, T. A. Cochran, D. Multer, M. Litskevich, Z. J. Cheng, X. P. Yang, Z. Guguchia, G. Xu, Z. Q. Wang, T. Neupert, S. D. Wilson, and M. Z. Hasan, Discovery of topological charge order in kagome superconductor KV_3Sb_5 , [arXiv:2012.15709](#).
- [8] S. Y. Yang, Y. J. Wang, B. R. Ortiz, D. F. Liu, J. Gayles, E. Derunova, R. Gonzalez-Hernandez, L. Šmejkal, Y. L. Chen, S. S. P. Parkin, S. D. Wilson, E. S. Toberer, T. McQueen, and M. N. Ali, Giant, unconventional anomalous Hall effect in the metallic frustrated magnet candidate, KV_3Sb_5 , *Sci. Adv.* **6**, eabb6003 (2020).
- [9] E. M. Kenney, B. R. Ortiz, C. N. Wang, S. D. Wilson, and M. J. Graf, Absence of local moments in the kagome metal KV_3Sb_5 as determined by muon spin spectroscopy, *J. Phys. Condens. Matter.* **33**, 235801 (2021).
- [10] H. Chen, H. T. Yang, B. Hu, Z. Zhao, J. Yuan, Y. Q. Xing, G. J. Qian, Z. H. Huang, G. Li, Y. H. Ye, Q. W. Yin, C. S. Gong, Z. J. Tu, H. C. Lei, S. Ma, H. Zhang, S. L. Ni, H. X. Tan, C. M. Shen, X. L. Dong, B. H. Yan, Z. Q. Wang, and H. J. Gao, Roton pair density wave and unconventional strong-coupling superconductivity in a topological kagome metal, [arXiv:2103.09188](#).
- [11] X. Chen, X. H. Zhan, X. J. Wang, J. Deng, X. B. Liu, X. Chen, J. G. Guo, and X. L. Chen, Highly-robust reentrant superconductivity in CsV_3Sb_5 under pressure, *Chin. Phys. Lett.* **38**, 057402 (2021).
- [12] M. M. Denner, R. Thomale, and T. Neupert, Analysis of charge order in the kagome metal AV_3Sb_5 ($A = K, Rb, Cs$), [arXiv:2103.14045](#).
- [13] F. Du, S. S. Luo, B. R. Ortiz, Y. Chen, W. Y. Duan, D. T. Zhang, X. Lu, S. D. Wilson, Y. Song, and H. Q. Yuan, Pressure-tuned interplay between charge order and superconductivity in the kagome metal KV_3Sb_5 , [arXiv:2102.10959](#).
- [14] W. Y. Duan, Z. Y. Nie, S. S. Luo, F. H. Yu, B. R. Ortiz, L. C. Yin, H. Su, F. Du, A. Wang, Y. Chen, X. Lu, J. J. Ying, S. D. Wilson, X. H. Chen, Y. Song, and H. Q. Yuan, Nodeless superconductivity in the kagome metal CsV_3Sb_5 , [arXiv:2103.11796](#).
- [15] X. L. Feng, K. Jiang, Z. Q. Wang, and J. P. Hu, Chiral flux phase in the kagome superconductor AV_3Sb_5 , [arXiv:2103.07097](#).
- [16] Y. Fu, N. N. Zhao, Z. Chen, Q. W. Yin, Z. J. Tu, C. S. Gong, C. Y. Xi, X. D. Zhu, Y. P. Sun, K. Liu, and H. C. Lei, Quantum transport evidence of topological band structures of kagome superconductor CsV_3Sb_5 , [arXiv:2104.08193](#).
- [17] H. Li, H. Zhao, B. R. Ortiz, T. Park, M. X. Ye, L. Balents, Z. Q. Wang, S. D. Wilson, and I. Zeljkovic, Rotation symmetry breaking in the normal state of a kagome superconductor KV_3Sb_5 , [arXiv:2104.08209](#).
- [18] H. X. Li, T. T. Zhang, Y.-Y. Pai, C. Marvinney, A. Said, T. Yilmaz, Q. Yin, C. Gong, Z. Tu, E. Vescovo, R. G. Moore, S. Murakami, H. C. Lei, H. N. Lee, B. Lawrie, and H. Miao, Observation of unconventional charge density wave without acoustic phonon anomaly in kagome superconductors AV_3Sb_5 ($A = Rb, Cs$), [arXiv:2103.09769](#).
- [19] Z. W. Liang, X. Y. Hou, W. R. Ma, F. Zhang, P. Wu, Z. Y. Zhang, F. H. Yu, J. J. Ying, K. Jiang, L. Shan, Z. Y. Wang, and X. H. Chen, Three-dimensional charge density wave and robust zero-bias conductance peak inside the superconducting vortex core of a kagome superconductor CsV_3Sb_5 , [arXiv:2103.04760](#).
- [20] Y. P. Lin and R. M. Nandkishore, Complex charge density waves at van Hove singularity on hexagonal lattices: Haldane-model phase diagram and potential realization in kagome metals AV_3Sb_5 , [arXiv:2104.02725](#).
- [21] Z. H. Liu, N. N. Zhao, Q. W. Yin, C. S. Gong, Z. J. Tu, M. Li, W. H. Song, Z. T. Liu, D. W. Shen, Y. B. Huang, K. Liu, H. C. Lei, and S. C. Wang, Temperature-induced band renormalization and Lifshitz transition in a kagome superconductor RbV_3Sb_5 , [arXiv:2104.01125](#).
- [22] C. Mu, Q. W. Yin, Z. J. Tu, C. S. Gong, H. C. Lei, Z. Li, and J. L. Luo, S -wave superconductivity in kagome metal CsV_3Sb_5 revealed by $^{121/123}Sb$ NQR and ^{51}V NMR measurements, [arXiv:2104.06698](#).
- [23] S. L. Ni, S. Ma, Y. H. Zhang, J. Yuan, H. T. Yang, Z. Y. W. Lu, N. N. Wang, J. P. Sun, Z. Zhao, D. Li, S. B. Liu, H. Zhang, H. Chen, K. Jin, J. G. Cheng, L. Yu, F. Zhou, X. L. Dong, J. P. Hu, H. J. Gao, and Z. X. Zhao, Anisotropic superconducting properties of kagome metal CsV_3Sb_5 , *Chin. Phys. Lett.* **38**, 057403 (2021).
- [24] N. Ratcliff, L. Hallett, B. R. Ortiz, S. D. Wilson, and J. W. Harter, Coherent phonon spectroscopy and interlayer modulation of charge density wave order in the kagome metal CsV_3Sb_5 , [arXiv:2104.10138](#).
- [25] H. X. Tan, Y. Z. Liu, Z. Q. Wang, and B. H. Yan, Charge density waves and electronic properties of superconducting kagome metals, [arXiv:2103.06325](#).
- [26] E. Uykur, B. R. Ortiz, O. Iakutkina, M. Wenzel, S. D. Wilson, M. Dressel, and A. A. Tsirlin, Low-energy optical properties of the non-magnetic kagome metal CsV_3Sb_5 , [arXiv:2104.14022](#).
- [27] Z. G. Wang, S. Ma, Y. H. Zhang, H. T. Yang, Z. Zhao, Y. Ou, Y. Zhu, S. L. Ni, Z. Y. W. Lu, H. Chen, K. Jiang, L. Yu, Y. Zhang, X. L. Dong, J. P. Hu, H. J. Gao, and Z. X. Zhao, Distinctive momentum dependent charge-density-wave gap observed in CsV_3Sb_5 superconductor with topological kagome lattice, [arXiv:2104.05556](#).
- [28] X. X. Wu, T. Schwemmer, T. Muller, A. Consiglio, G. Sangiovanni, D. D. Sante, Y. Iqbal, W. Hanke, A. P. Schnyder, M. M. Denner, M. H. Fisher, T. Neupert, and R. Thomale, Nature of unconventional pairing in the kagome superconductors AV_3Sb_5 , [arXiv:2104.05671](#).
- [29] Y. Xiang, Q. Li, Y. K. Li, X. W., H. Yang, Z. W. Wang, Y. G. Yao, and H. H. Wen, Nematic electronic state and twofold symmetry of superconductivity in the topological kagome metal CsV_3Sb_5 , [arXiv:2104.06909](#).
- [30] F. H. Yu, T. Wu, Z. Y. Wang, B. Lei, W. Z. Zhuo, J. J. Ying, and X. H. Chen, Concurrence of anomalous Hall effect and charge density wave in a superconducting topological kagome metal, [arXiv:2102.10987](#).
- [31] Z. Y. Zhang, Z. Chen, Y. Zhou, Y. F. Yuan, S. Y. Wang, L. L. Zhang, X. D. Zhu, Y. H. Zhou, X. L. Chen, J. H. Zhou, and Z. R. Yang, Pressure-induced reemergence of superconductivity in topological kagome metal CsV_3Sb_5 , [arXiv:2103.12507](#).

- [32] H. Zhao, H. Li, B. R. Ortiz, S. M. L. Teicher, T. Park, M. X. Ye, Z. Q. Wang, L. Balents, S. D. Wilson, and I. Zeljkovic, Cascade of correlated electron states in a kagome superconductor CsV_3Sb_5 , [arXiv:2103.03118](#).
- [33] J. Z. Zhao, W. K. Wu, Y. L. Wang, and S. Y. A. Yang, Electronic correlations in the normal state of kagome superconductor KV_3Sb_5 , [arXiv:2103.15078](#).
- [34] X. X. Zhou, Y. K. Li, X. W. Fan, J. H. Hao, Y. M. Dai, Z. W. Wang, Y. G. Yao, and H. H. Wen, Origin of the charge density wave in the kagome metal CsV_3Sb_5 as revealed by optical spectroscopy, [arXiv:2104.01015](#).
- [35] S. L. Yu and J. X. Li, Chiral superconducting phase and chiral spin-density-wave phase in a Hubbard model on the kagome lattice, *Phys. Rev. B* **85**, 144402 (2012).
- [36] M. Leroux, V. Mishra, J. P. C. Ruff, H. Claus, M. P. Smylie, C. Opagiste, P. Rodiere, A. Kayani, G. D. Gu, J. M. Tranquada, W. K. Kwok, Z. Islam, and U. Welp, Disorder raises the critical temperature of a cuprate superconductor, *Proc. Natl. Acad. Sci. U.S.A.* **116**, 10691 (2019).
- [37] M. Leroux, V. Mishra, C. Opagiste, P. Rodière, A. Kayani, W. K. Kwok, and U. Welp, Charge density wave and superconductivity competition in $\text{Lu}_3\text{Ir}_4\text{Si}_{10}$: A proton irradiation study, *Phys. Rev. B* **102**, 094519 (2020).
- [38] J. P. Sun, K. Matsuura, G. Z. Ye, Y. Mizukami, M. Shimozawa, K. Matsubayashi, M. Yamashita, T. Watashige, S. Kasahara, Y. Matsuda, J. Q. Yan, B. C. Sales, Y. Uwatoko, J. G. Cheng, and T. Shibauchi, Dome-shaped magnetic order competing with high-temperature superconductivity at high pressures in FeSe , *Nat. Commun.* **7**, 12146 (2016).
- [39] Y. Uwatoko, S. Todo, K. Ueda, A. Uchida, M. Kosaka, N. Mori, and T. Matsumoto, Material properties of Ni–Cr–Al alloy and design of a 4 GPa class non-magnetic high-pressure cell, *J. Phys. Condens. Matter* **14**, 11291 (2002).
- [40] J. G. Cheng, K. Matsubayashi, S. Nagasaki, A. Hisada, T. Hirayama, M. Hedo, H. Kagi, and Y. Uwatoko, Integrated-fin gasket for palm cubic-anvil high pressure apparatus, *Rev. Sci. Instrum.* **85**, 093907 (2014).
- [41] See Supplemental Material at <http://link.aps.org/supplemental/10.1103/PhysRevLett.126.247001> for experimental and computational details, which includes Refs. [3,39,40,42–49].
- [42] V. G. Kogan and R. Prozorov, Orbital upper critical field and its anisotropy of clean one- and two-band superconductors, *Rep. Prog. Phys.* **75**, 114502 (2012).
- [43] J. Zaanen, Quantum critical electron systems: The uncharted sign worlds, *Science* **319**, 1205 (2008).
- [44] P. E. Blöchl, Projector augmented-wave method, *Phys. Rev. B* **50**, 17953 (1994).
- [45] W. Kohn and L. J. Sham, Self-consistent equations including exchange and correlation effects, *Phys. Rev.* **140**, A1133 (1965).
- [46] G. Kresse and J. Furthmüller, Efficient iterative schemes for ab initio total-energy calculations using a plane-wave basis set, *Phys. Rev. B* **54**, 11169 (1996).
- [47] J. P. Perdew, K. Burke, and M. Ernzerhof, Generalized Gradient Approximation Made Simple, *Phys. Rev. Lett.* **77**, 3865 (1996).
- [48] S. Grimme, J. Antony, S. Ehrlich, and H. Krieg, A consistent and accurate ab initio parametrization of density functional dispersion correction (DFT-D) for the 94 elements H–Pu, *J. Chem. Phys.* **132**, 154104 (2010).
- [49] S. Grimme, S. Ehrlich, and L. Goerigk, Effect of the damping function in dispersion corrected density functional theory, *J. Comput. Chem.* **32**, 1456 (2011).
- [50] P. Monceau, N. P. Ong, A. M. Portis, A. Meerschaut, and J. Rouxel, Electric Field Breakdown of Charge-Density-Wave-Induced Anomalies in NbSe_3 , *Phys. Rev. Lett.* **37**, 602 (1976).
- [51] J. Chaussy, P. Haen, J. C. Lasjaunias, P. Monceau, G. Waysand, A. Waintal, A. Meerschaut, P. Molinié, and J. Rouxel, Phase transitions in NbSe_3 , *Solid State Commun.* **20**, 759 (1976).
- [52] A. F. Kusmartseva, B. Sipos, H. Berger, L. Forró, and E. Tutiš, Pressure Induced Superconductivity in Pristine $1T\text{-TiSe}_2$, *Phys. Rev. Lett.* **103**, 236401 (2009).
- [53] O. Moulding, I. Osmond, F. Flicker, T. Muramatsu, and S. Friedemann, Absence of superconducting dome at the charge-density-wave quantum phase transition in $2H\text{-NbSe}_2$, *Phys. Rev. Research* **2**, 043392 (2020).
- [54] T. Wu, H. Mayaffre, S. Krämer, M. Horvatić, C. Berthier, W. N. Hardy, R. X. Liang, D. A. Bonn, and M. H. Julien, Magnetic-field-induced charge-stripe order in the high-temperature superconductor $\text{YBa}_2\text{Cu}_3\text{O}_y$, *Nature (London)* **477**, 191 (2011).
- [55] H. Q. Yuan, F. M. Grosche, M. Deppe, C. Geibel, G. Sparn, and F. Steglich, Observation of two distinct superconducting phases in CeCu_2Si_2 , *Science* **302**, 2104 (2003).
- [56] B. Keimer, S. A. Kivelson, M. R. Norman, S. Uchida, and J. Zaanen, From quantum matter to high-temperature superconductivity in copper oxides, *Nature (London)* **518**, 179 (2015).
- [57] P. Shahi, J. P. Sun, S. H. Wang, Y. Y. Jiao, K. Y. Chen, S. S. Sun, H. C. Lei, Y. Uwatoko, B. S. Wang, and J. G. Cheng, High- T_c superconductivity up to 55 K under high pressure in a heavily electron doped $\text{Li}_{0.36}(\text{NH}_3)_y\text{Fe}_2\text{Se}_2$ single crystal, *Phys. Rev. B* **97**, 020508(R) (2018).
- [58] J. P. Sun, P. Shahi, H. X. Zhou, Y. L. Huang, K. Y. Chen, B. S. Wang, S. L. Ni, N. N. Li, K. Zhang, W. G. Yang, Y. Uwatoko, G. Xing, J. Sun, D. J. Singh, K. Jin, F. Zhou, G. M. Zhang, X. L. Dong, Z. X. Zhao, and J. G. Cheng, Reemergence of high- T_c superconductivity in the $(\text{Li}_{1-x}\text{Fe}_x)\text{OHFe}_{1-y}\text{Se}$ under high pressure, *Nat. Commun.* **9**, 380 (2018).
- [59] J. P. Sun, M. Z. Shi, B. Lei, S. X. Xu, Y. Uwatoko, X. H. Chen, and J. G. Cheng, Pressure-induced second high- T_c superconducting phase in the organic-ion-intercalated $(\text{CTA})_{0.3}\text{FeSe}$ single crystal, *Europhys. Lett.* **130**, 67004 (2020).
- [60] T. Gruner, D. J. Jang, Z. Huesges, R. Cardoso-Gil, G. H. Fecher, M. M. Koza, O. Stockert, A. P. Mackenzie, M. Brando, and C. Geibel, Charge density wave quantum critical point with strong enhancement of superconductivity, *Nat. Phys.* **13**, 967 (2017).
- [61] J. H. Chu, H. H. Kuo, J. G. Analytis, and I. R. Fisher, Divergent nematic susceptibility in an iron arsenide superconductor, *Science* **337**, 710 (2012).
- [62] N. Barisic, M. K. Chan, Y. Li, G. Yu, X. Zhao, M. Dressel, A. Smontara, and M. Greven, Universal sheet resistance and

- revised phase diagram of the cuprate high-temperature superconductors, *Proc. Natl. Acad. Sci. U.S.A.* **110**, 12235 (2013).
- [63] J. C. Davis and D. H. Lee, Concepts relating magnetic interactions, intertwined electronic orders, and strongly correlated superconductivity, *Proc. Natl. Acad. Sci. U.S.A.* **110**, 17623 (2013).
- [64] L. Zhao, C. A. Belvin, R. Liang, D. A. Bonn, W. N. Hardy, N. P. Armitage, and D. Hsieh, A global inversion-symmetry-broken phase inside the pseudogap region of $\text{YBa}_2\text{Cu}_3\text{O}_y$, *Nat. Phys.* **13**, 250 (2017).
- [65] W. C. Yu, Y. W. Cheung, P. J. Saines, M. Imai, T. Matsumoto, C. Michioka, K. Yoshimura, and S. K. Goh, Strong Coupling Superconductivity in the Vicinity of the Structural Quantum Critical Point in $(\text{Ca}_x\text{Sr}_{1-x})_3\text{Rh}_4\text{Sn}_{13}$, *Phys. Rev. Lett.* **115**, 207003 (2015).
- [66] Y. Nakajima, H. Shishido, H. Nakai, T. Shibauchi, K. Behnia, K. Izawa, M. Hedo, Y. Uwatoko, T. Matsumoto, R. Settai, Y. Ōnuki, H. Kontani, and Y. Matsuda, Non-Fermi liquid behavior in the magnetotransport of CeMIn_5 (M : Co and Rh): Striking similarity between quasi two-dimensional heavy fermion and high- T_c cuprates, *J. Phys. Soc. Jpn.* **76**, 024703 (2007).